ELSEVIER

Journal of Molecular Catalysis A: Chemical 176 (2001) 213–226

JOURNAL OF MOLECULAR CATALYSIS A: CHEMICAL

www.elsevier.com/locate/molcata

The synergism of cadmium on the catalytic activity of Cd–Cr–O system I. Preparation, characterization and electrical properties

A.M. El-Awad*, B.M. Abu-Zied

Chemistry Department, Faculty of Science, Assiut University, 71516 Assiut, Egypt

Received 24 February 2001; accepted 6 June 2001

Abstract

Cadmium-containing catalysts were obtained by calcining a parent mixture of chromia and cadmium nitrate precursor materials in atomic ratio Cd/Cr = 0.5. The thermal genesis of the catalysts was explored by means of thermogravimetric analysis (TGA) in different atmospheres (air, nitrogen, and hydrogen) and in the temperature range 25–1000°C. The calcination products were characterized by adopting many techniques such as differential scanning calorimetry (DSC), Fourier transform infrared spectroscopy (FTIR), scanning electron microscopy (SEM), estimation of surface excess Cr^{6+} concentration, surface area, and electrical conductivity measurements. It was demonstrated that raising the calcination temperature of Cd/Cr mixture results in many effects on the structural as well as the electrical properties of the calcination products. The role of Cd^{2+} ions in improving the electrical behavior of such a mixture was discussed. The results of the present study offer the advantageously usage of Cd/Cr catalysts over the net chromia catalyst in the dehydration/dehydrogenation of alcohols as it will be discussed in the next paper.

Keywords: Spinels; Chromium oxide; Cadmium chromate and chromite; Electrical conductivity

1. Introduction

Chromia possesses an interesting electrical, magnetic as well as surface properties that affect its usage as an industrial catalyst in many reactions. Such reactions include oxidative dehydrogenation of isobutane [1] and ethane [2], selective oxidation of H_2S [3], CO oxidation [4] and ethylene polymerization [5]. When annealing takes place, in air, the gel suffers the well-known oxidation–reduction cycle ($Cr^{3+} \rightarrow Cr^{6+} \rightarrow Cr^{3+}$) and becoming a highly nonstoichiometric oxide [6]. The presence of chromium ions in various oxidation states enables an easy exchange of electrons between the oxide and the adsorbed species of the catalytic reactions, the oxide being in a position to accept electrons as well as to give them up. This means that both the adsorptive and the catalytic properties of the gel are sensitive to the conditions of preparation and heat treatment. Chromia can be considered as a host oxide in preparing many groups of catalysts, viz. solid solutions, perovskites, and spinels. Considering its industrial importance [7], metal chromites, MCr_2O_4, represent another example for the previously mentioned redox cycle. In addition to the preparation procedure and according to Fahim et al. [8] this cycle is controlled by the extent to which the divalent cation (M) can exchange electrons with the surface chromia ions. Recent

* Corresponding author. Tel.: +20-88-412107; fax: +20-88-342708.
E-mail address: el-awad@aun.eun.eg (A.M. El-Awad).

1381-1169/01/$ – see front matter
PII: S1381-1169(01)00262-X

investigations performed in our laboratory [9–11] have concerned with the effect of addition of alkaline earth as well as some transition metal cations on the formation and stability of chromate/chromite systems. Among the investigated systems, Zn–Cr–O system showed interesting features. Reviewing the literature revealed that a great number of publications have been reported on the formation [12–14], characterization [7,14–17], and catalytic behavior [18–21] of stoichiometric and non-stoichiometric zinc chromite spinel.

The chemistry of zinc and cadmium is very similar [22]. Moreover, they naturally occur together [23]. To our knowledge, in the last two decades, no studies on the catalytic properties of $CdCrO_4$ or $CdCr_2O_4$ systems have been reported. From this point of view, it is of interest to investigate the textural as well as the catalytic properties of the calcination products of cadmium-containing chromia catalysts. Therefore, the present paper was undertaken to shed some light on the textural and electrical conduction variations accompanying the heat treatment, in different atmospheres, of a mixture of cadmium nitrate and chromia gel ($CdO:Cr_2O_3$ molar ratio) from ambient up to 1000°C. Characterization was carried out by using different techniques, thermal analyses, viz. thermogravimetric analysis (TGA) and differential scanning calorimetry (DSC), X-ray diffractometry (XRD), Fourier transform infrared spectroscopy (FTIR), and scanning electron microscopy (SEM). In addition, surface area of different calcination products was determined using nitrogen adsorption at −196°C. Moreover, water extractable Cr^{6+} ions estimation and electrical conductivity measurements were also carried out. In a next paper, the catalytic behavior of the calcination products, as obtained in the temperature range 400–1000°C, towards ethanol decomposition will be discussed on the basis of their structural as well as electrical properties.

2. Experimental

2.1. Apparatus and techniques

TGA and DSC analyses were performed on the parent cadmium/chromia mixture using thermal analyst TA-2000 apparatus. The effect of the surrounding atmosphere on the thermal behavior of cadmium/chromia parent was followed throughout TGA analysis by heating the starting mixture from ambient up to 1000°C in a dynamic atmosphere (40 ml min^{-1}) of air, nitrogen, and hydrogen.

XRD patterns were recorded using a Philips diffractometer (type PW 2103/00). The Philips generator, operated at 35 kV and 20 mA, provided a source of Cu Kα radiation. FTIR spectra were obtained using KBr disk technique over the range 1200–400 cm^{-1} at a resolution of 2 cm^{-1} using Nicolet 710 FTIR spectrophotometer. Disks containing 2 mg of each sample and 200 mg of KBr (spectroscopically pure) were prepared for comparable purpose.

Water extractable Cr^{6+} ion concentrations were determined spectrophotometrically [9]. The measurements were made on a Shimadzu UV-200S double beam spectrophotometer. Surface areas were determined by BET analysis of the corresponding nitrogen adsorption isotherms (measured at −196°C) [24]. The isotherms were obtained by using Quantachrome (Nova 3200 series) multigas adsorption apparatus. Scanning electron micrographs were obtained using a JEOL scanning microscope, model JSM-5400 LV. The samples were prepared by the gold sputtering technique [25].

The electrical conductivity measurements, adopting the pellet technique, were carried out using a conductivity cell described by Chapman et al. [26]. The temperature was controlled with a Cole–Parmer temperature controller (type Digi-Sense). The resistance measurements were carried out using a Keithley instrument 610 solid-state electrometer.

2.2. Catalysts preparation

Analytical grade chemicals were used. Chromia gel was prepared [27] by adding chromium nitrate solution (0.1 M) with constant stirring. The complete precipitation was performed at pH = 9.1. The precipitate was left overnight, filtered using centrifuge, then washed twice with distilled water, finally dried at 100°C until constant weight. The cadmium/chromia mixture ($CdO:Cr_2O_3$ molar ratio) was prepared following the impregnation procedure reported elsewhere [28]. Finally, and based on the thermal analysis results, the parent mixture as well as chromia gel parent were calcined in air at 300–1000°C temperature range, for 5 h, then quenched to room temperature. For simplicity,

the catalysts will be referred to by abbreviations Cr-*x* and Cd/Cr-*x*, for chromia gel and the mixture respectively, where *x* indicates the calcination temperature.

3. Results and discussion

3.1. TGA and DSC analyses

TGA thermograms of the solid mixture chromia/cadmium nitrate parent mixture, as obtained in air, pure nitrogen and hydrogen atmospheres are shown in Fig. 1, thermograms a–c, respectively. The obtained TGA curve in air atmosphere (Fig. 1a) shows

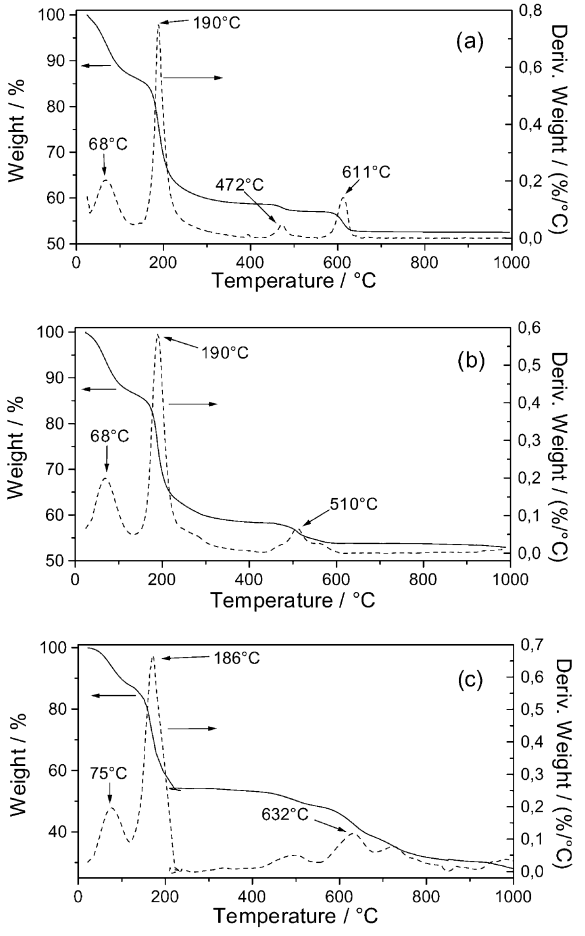

Fig. 1. TGA and DTG curves obtained by heating (at 10°C min^{-1}) the cadmium/chromia parent mixture in dynamic atmosphere (40 ml min^{-1}) of air (a), nitrogen (b), and hydrogen (c).

three main stages. The completion of the first stage is obtained at 250°C and corresponds to 47.7% weight loss (WL). This stage seems to be a composite one, which involves two different processes taking place simultaneously, viz. the decomposition of the parent constituents of the mixture and the solid-state reaction, which eventually leads to the formation of some solid products. These products will be identified later. The other two stages lie in the temperature range 440–520 and 570–665°C with the corresponding WL of 1.64 and 4.5%. In order to identify the different solid phases at each stage, the parent mixture was isothermally heated at 250, 520 and 665°C for 20 min, which are the temperatures corresponding to the completion of stages 1–3 respectively (as detected from the DTG plot in Fig. 1a). XRD analysis of the solid products revealed the existence of α-$CdCrO_4$ together with CrOOH, α-Cr_2O_3 with β-$CdCrO_4$, and $CdCr_2O_4$ [29] as the major phases in stages 1–3, respectively. According to our results, cadmium chromate suffers a phase transition in the 400–500°C temperature range. Such transformation will be discussed later (cf. XRD results). Based on the obtained WL values corresponding to the different stages and with the aid of XRD analysis, the thermal behavior of the parent mixture, in air, can be described as follows:

$$\text{Parent} \overset{250^\circ\text{C}}{\rightarrow} \alpha\text{-}CdCrO_4 + CrOOH + \text{gases} \quad (1)$$

$$\alpha\text{-}CdCrO_4 \overset{400\text{–}500^\circ\text{C}}{\rightarrow} \beta\text{-}CdCrO_4 \quad (2)$$

$$CrOOH \overset{440\text{–}520^\circ\text{C}}{\rightarrow} \tfrac{1}{2}\alpha\text{-}Cr_2O_3 + \tfrac{1}{2}H_2O \quad (3)$$

$$\beta\text{-}CdCrO_4 + \tfrac{1}{2}\alpha\text{-}Cr_2O_3 \overset{665^\circ\text{C}}{\rightarrow} CdCr_2O_4 + \tfrac{3}{4}O_2 \quad (4)$$

When the decomposition was performed in nitrogen atmosphere, the TGA curve of the parent mixture showed two main stages (Fig. 1b). The first stage is identical with that found in case of heating the parent mixture in air, while the second stage lies in the 440–580°C temperature range and corresponds to 5.28% WL. Results of XRD analysis confirmed the formation of α-$CdCrO_4$ together with CrOOH in the first stage whereas $CdCr_2O_4$ is the only detected product at the end of the second stage. Thus, the thermal behavior of the parent mixture in nitrogen atmosphere may be expressed as follows:

$$\text{Parent} \overset{250^\circ\text{C}}{\rightarrow} \alpha\text{-}CdCrO_4 + CrOOH + \text{gases} \quad (5)$$

$$\alpha\text{-}CdCrO_4 + CrOOH \xrightarrow{440-580^\circ C} CdCr_2O_4 + \tfrac{1}{2}H_2O + \tfrac{3}{4}O_2 \quad (6)$$

On the other hand, the TGA curve in hydrogen atmosphere (Fig. 1c) seems to be completely different compared with those obtained in air or nitrogen. It shows two main stages, the completion of the first one takes place at 220°C and corresponds to 47.56% WL, whereas the second stage takes place along a very wide range of temperatures (500–850°C) and corresponds to 23.85% WL value. Using the same method of phase identification, as previously mentioned in case of air and nitrogen atmospheres, it was found that $CdCr_2O_4$ and α-Cr_2O_3 are the only solid products formed at the end of stages 1 and 2, respectively. Accordingly, it can be concluded that the role of hydrogen atmosphere is to accelerate the formation of $CdCr_2O_4$ phase at relatively lower temperatures, whereas at higher temperatures, above 500°C, it causes the decomposition of the spinel with the complete reduction of Cd^{2+} ions to zerovalent cadmium. In this context, it is worth-mentioning that the total WL value in the second stage which amounts to 23.85% is very close to that anticipated theoretically to the removal of cadmium oxide. This fact together with the XRD analysis, which indicates the presence of Cr_2O_3 as the only phase detected at the end of stage 2, enable us to suggest that the second stage proceeds as follows:

$$CdCr_2O_4 + H_2 \xrightarrow{500-850^\circ C} Cr_2O_3 + Cd\uparrow + H_2O\uparrow \quad (7)$$

It is obvious that the produced Cd metal will evaporate at temperature higher than 660°C [30]; leaving Cr_2O_3 as the only solid phase exists; offering a theoretical WL value (24.8%), a situation agrees well with that found in TGA analysis (Fig. 1c).

Aiming to evaluate the kinetic parameters as well as the rate equations describing the thermal behavior of the parent mixture in the various atmospheres, the α-temperature data (where α is the fraction decomposed) were analyzed using a computer program [31] and by applying the two methods, Coats–Redfern and Horowitz–Metzger. The obtained results as depicted in Table 1 show that the phase boundary movement model (F_2), where $F_2(\alpha) = -[1-(1-\alpha)^{-1}]$, is the one which gives the best fit of data in both air and nitrogen atmospheres. This model changes to become the three-dimensional diffusion model (D_3) [32], where $D_3(\alpha) = 1.5[1-(1-\alpha)^{1/3}]^2$, in hydrogen atmosphere. On the other hand, a comparison between the calculated activation energy values (E_a) in the 140–250°C temperature range, corresponding to stage 1, indicates that the reaction atmosphere significantly influences these values. It shows a greater E_a values in case of nitrogen than in air atmosphere. This result may be related to the formation of cadmium chromate phase in stage 1. The formation of such a phase involves the oxidation reaction $Cr^{3+} \rightarrow Cr^{6+}$ that is greatly enhanced in air atmosphere offering such a lowering in E_a value. It is to be noticed that the above explanation cannot be applied in case of using hydrogen atmosphere. In such a case, the chromite phase is directly formed in stage 1 instead of chromate one. When a comparison between the E_a values was held in the temperature range corresponding to the decomposition of $CdCrO_4$ into $CdCr_2O_4$ phase, it was found that the activation energy value in presence of air becomes much greater (212 kcal mol^{-1}) compared with that in nitrogen atmosphere (76.1 kcal mol^{-1}), a situation that may be related to the retarding effect of oxygen on the transformation process of $CdCrO_4$ to $CdCr_2O_4$ phase which involves the reduction reaction

Table 1
Activation energy values of the decomposition of the Cd/Cr parent mixture in different atmospheres

Atmosphere	Stage	Coats–Redfern			Horowitz–Metzger		
		E_a (kcal mol^{-1})	log A	Model	E_a (kcal mol^{-1})	log A	Model
Air	1	8.9	2.14	F_2	17.4	6.04	F_2
	2	212	24.5	F_2	210.6	36.6	F_2
Nitrogen	1	28.8	6.9	F_2	28.5	11.5	F_2
	2	76.1	10.5	F_2	79.2	20.15	F_2
Hydrogen	1	20.3	4.68	D_3	4.5	0.45	D_3

$Cr^{6+} \rightarrow Cr^{3+}$. In this respect, it was stated [33] that the activation process for the thermal decomposition of solid chromates is a one-electron transfer from the nonbonding oxygen π-orbital to the chromium ($t_1 \rightarrow$ 2e electronic transition). The activation energy for the thermal decomposition of chromates may be related to the energy of this charge transfer process; the effect of this is to reduce the oxidation state of chromium from +6 to +5, then a strong polarization effect of cations leading to further reduction of Cr^{5+} to Cr^{3+} occurs [33]. From this point of view and as a probe to recognize the various stages of the decomposition of the parent mixture, in situ measurements of the electrical conductivity were performed in the two atmospheres, air and hydrogen. The results as conducted in the 25–500°C temperature range (500°C is the temperature limit for measuring in our conductivity cell) are shown in Fig. 2a and b, respectively, as $\log\sigma$ versus temperature relationship. The obtained plot (Fig. 2a) is divided into many regions, I–VIII, which are; from point I to II, the conductance is slightly increased due to thermal energy causing electrons emitting from low energy level to conduction band [34]. From point II to III, the lowering in the conductance may be attributed [35] to the removal of water according to

$$Cr(OH)_3 \rightarrow CrOOH + H_2O \quad (8)$$

From point III to IV and then to point V, the two dominant reactions in this region of temperature are, respectively, the decomposition of cadmium nitrate and the formation of α-$CdCrO_4$. It is obvious that the formation of the later phase, which involves the oxidation process, $Cr^{3+} \rightarrow Cr^{6+} + 3e^-$, is responsible for the large conductivity increase in the IV–V region throughout increasing the number of charge carriers. From point V to VI, the obtained values show the temperature-dependence of the conductivity behavior of the formed α-$CdCrO_4$ phase. In addition, the phase transition process of α- to β-$CdCrO_4$ as well as α-Cr_2O_3 formation are responsible for the noticeable lowering of conductivity in the region VI–VII. After the completion of these processes, the electrical conductivity of solid product behaves a continuous increase with increasing the temperature up to 500°C (point VIII). It is worth-noting that the above explanation is in a complete agreement with both TGA (Fig. 1a) and DSC (vide infra) results. It also finds further support when the conductivity measurements were conducted in hydrogen atmosphere (Fig. 2b). In such a case, the obtained conductivity behavior clearly indicates the absence of the characteristic effects above 400°C. These effects were related before (Fig. 2a) to α-Cr_2O_3 formation. Instead, a sharp conductivity lowering was found which could be ascribed to the direct formation of $CdCr_2O_4$ phase in the reducing atmosphere.

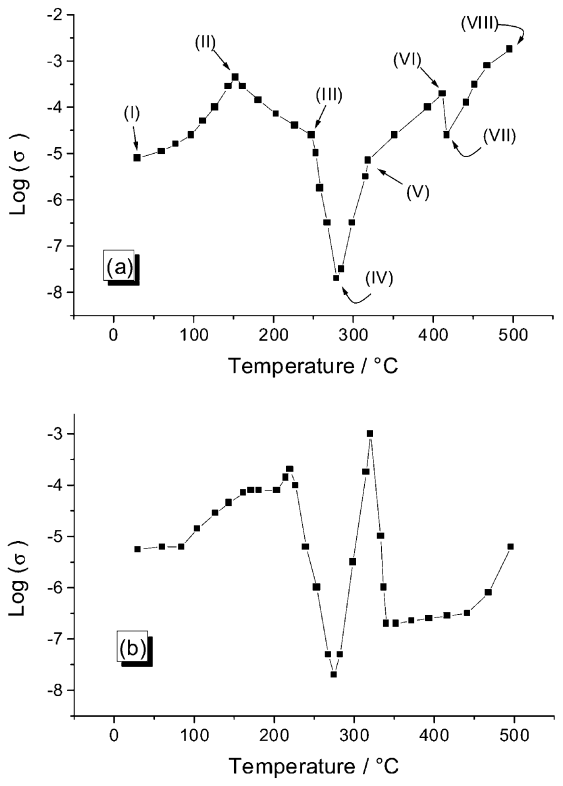

Fig. 2. Variation of $\log\sigma$ with temperature during heating (at 10°C min^{-1}) the parent cadmium/chromia mixture in air (a) and hydrogen (b) atmospheres.

DSC thermogram obtained for the parent mixture in air is shown in Fig. 3. The heating curve (solid curve) manifests four endothermic effects maximized at 45, 142, 193, and 599°C together with other three exothermic peaks located at 184, 428, and 487°C. The early two endothermic effects are corresponding to the elimination of different types of water of hydration [36], followed by an exothermic effect at 184°C which has been attributed to the formation of CrOOH [36]. The main endothermic peak at 193°C seems to

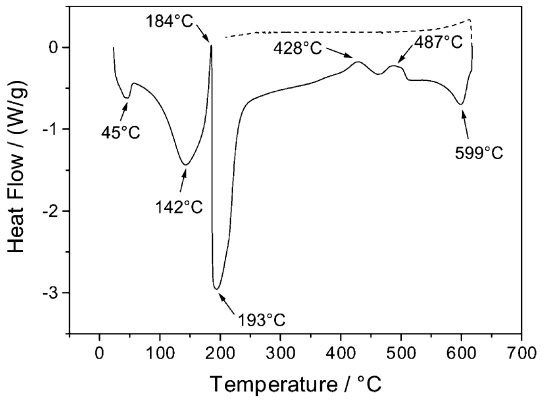

Fig. 3. DSC thermogram for heating (solid curve) and cooling (dashed curve) the cadmium/chromia parent (at $10^{\circ}C\,min^{-1}$).

be not a simple one, it is a composite peak involves two processes: (i) decomposition of cadmium nitrate, and (ii) solid-state reaction leading eventually to the formation of α-$CdCrO_4$ phase, such process involves the oxidation reaction $Cr^{3+} \rightarrow Cr^{6+}$. The second exothermic peak at 428°C refers to the crystallization of orthorhombic CrOOH into α-structure, which is accompanied by water evolution, as indicated by TGA analysis [10,37]. The last exothermic effect at 487°C can be assigned to the α- to β-$CdCrO_4$ phase transition. Such process is confirmed by XRD analysis (vide infra). Finally, the endothermic peak being located at 599°C is referred to the decomposition of chromate phase to chromite one. It is worth-mentioning that the previously discussed thermal events are irreversible, a fact which can be clearly understood by checking the cooling curve of the parent mixture (Fig. 3, dashed curve). Based on the above TGA analysis, the parent mixture was isothermally calcined in air, for 5 h, in the 300–1000°C temperature range. The structural as well as the electrical properties of the obtained samples will be given in the next sections.

3.2. X-ray diffraction (XRD) analysis

The XRD patterns of the calcination products of Cr/Cd mixture in the temperature range 300–1000°C are presented in Fig. 4 and summarized in Table 2. Results of Cr/Cd-300 revealed the existence of two major phases, viz. α-$CdCrO_4$ and CrOOH [29], whereas Cr/Cd-400 showed the coexistence of both α-$CdCrO_4$ (major) and α-Cr_2O_3 (minor). The detection of α-Cr_2O_3 agrees well with the reported data [38–40] concerning the formation of microcrystallites of α-Cr_2O_3 at 400°C. Raising the calcination temperature up to 500°C is accompanied by a phase transition of $CdCrO_4$ from α- to β-structure. On the other hand, the pattern of Cd/Cr-600 catalyst undergoes remarkable structural changes. Our analysis showed that cadmium chromite phase (major) together with chromic oxide (minor) and cadmium chromate (trace) represent the constituents of Cd/Cr-600 catalyst. Further rise of the calcination temperature up to 700°C leads to progressive formation of $CdCr_2O_4$ at the expense of the other phases. The picture for Cd/Cr-1000 catalyst is almost the same as that of Cd/Cr-700. Only the intensity of the characteristic lines of the former become sharper reflecting an increase of the crystallinity order.

From the absence of the characteristic lines of CdO together with the detection of α-Cr_2O_3 and β-$CdCrO_4$ phases in trace amounts in the XRD patterns for the samples calcined in the 700–1000°C temperature range, we can conclude that the spinel is formed immediately as a result of the decomposition of cadmium chromate according to

$$2\beta\text{-}CdCrO_4 \rightarrow CdCr_2O_4 + CdO + \tfrac{3}{2}O_2 \qquad (9)$$

This coincides with our earlier results for the thermal stability of zinc chromate [9]. The newly formed CdO phase in Eq. (9) reacts, simultaneously, with excess α-Cr_2O_3 (minor phase in Cd/Cr-500 catalyst) to form another molecule of cadmium chromite spinel according to

$$CdO + \alpha\text{-}Cr_2O_3 \rightarrow CdCr_2O_4 \qquad (10)$$

In view of this conclusion, the thermal behavior given by the above two equations can be represented as a whole by Eq. (4). The parent chromia gel was subjected to the same heat treatment in the 400 up to 1000°C temperature range. XRD investigations of the obtained samples (the data are not shown) revealed that all the diffraction peaks for all samples were assigned to α-Cr_2O_3 (with d (Å) = 2.48, 2.67, and 1.67), while no peaks for other compounds such as CrO_2 and CrO_3 were detected in the diffraction diagrams.

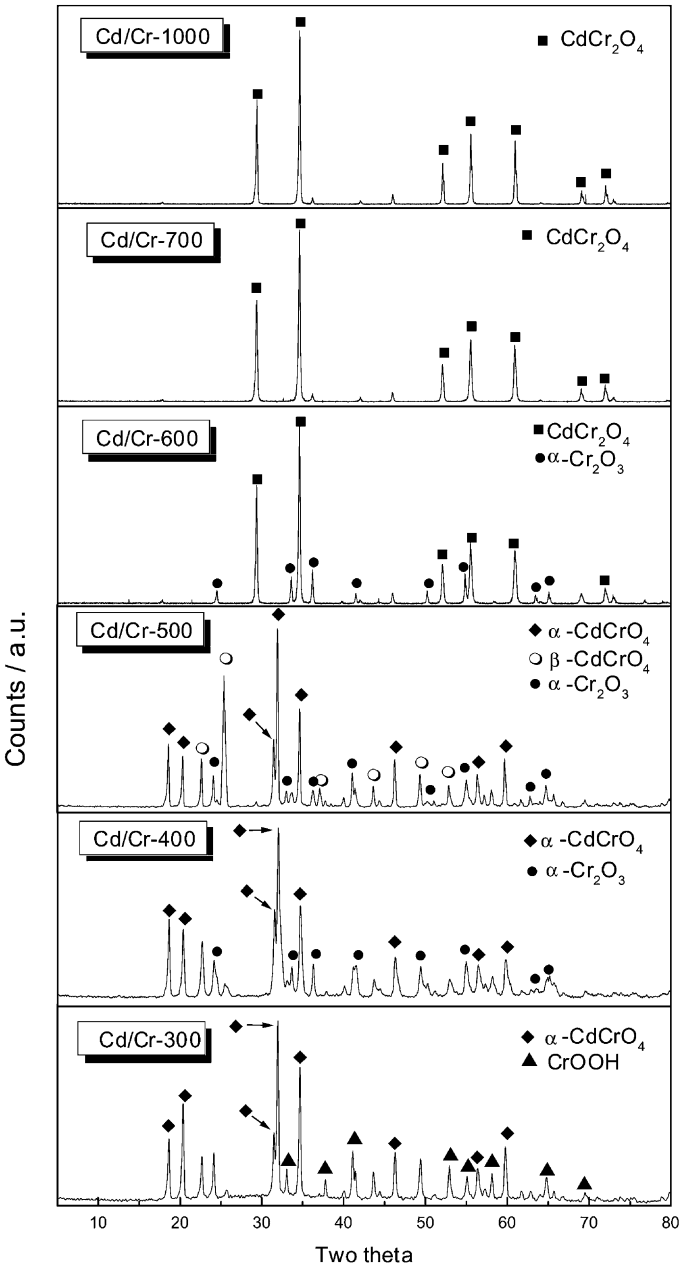

Fig. 4. XRD powder diffractograms for the calcination products of the parent cadmium/chromia mixture in the temperature range 300–1000°C.

3.3. FTIR spectra

The FTIR spectra taken for the calcination products of the parent cadmium/chromia mixture are shown in Fig. 5. The spectrum of the starting sample, i.e. Cd/Cr-300, shows absorptions at 923(s), 867(w), 827(sh), 799(s), 533(b), and 423(w) cm^{-1}, where s = sharp, w = weak, sh = shoulder, and b = broad.

Table 2
Structural information of calcined cadmium/chromia mixture[a]

Calcination temperature (°C)	Phase detected				
	α-Cr_2O_3	α-$CdCrO_4$	β-$CdCrO_4$	$CdCr_2O_4$	CrOOH
300	–	j	–	–	m
400	m	j	–	–	–
500	m	j	j	–	–
600	m	–	t	j	–
700	t	–	–	j	–
1000	t	–	–	J	–

[a] j: major, m: minor, and t: trace.

The early two bands at 533 and 423 cm^{-1} are due to lattice vibration of chromium oxide [6,37,41–44]. The bands located in the spectral region 930–780 cm^{-1}, which cover the fundamental frequencies of normal chromates [10,16,43–45], can be assigned according to Muller et al. [46] to different stretching vibrations of α-$CdCrO_4$. The FTIR spectrum of the parent mixture calcined at 400°C shows a progressive increase in the intensity of the absorption bands due to α-$CdCrO_4$. In addition, the band located at 923 cm^{-1}, for Cd/Cr-300 catalyst, is splitted into two bands at 927 and 907 cm^{-1}. On the other hand, in the low frequency region (at $<700\,cm^{-1}$, where the absorption due to Cr^{3+}–O vibrations appears) one can observe that the band at 533 cm^{-1} is splitted into two bands at 627 and 583 cm^{-1}. Meanwhile, a new band at 465 cm^{-1} emerged. Such absorptions are assigned to α-Cr_2O_3 [37,42]. The FTIR spectrum of the calcination products at 500°C is in line with the XRD results (Table 2). This is clearly manifested by the persistence of the previously detected bands characterizing α-$CdCrO_4$ and α-Cr_2O_3. Moreover, a new band located at 765 cm^{-1} appeared, which can be assigned to the presence of β-$CdCrO_4$ [46]. It is worth-mentioning that this newly detected band lies in the 840–720 cm^{-1} wavenumber region, where the Cr–O–Cr stretching vibration of dichromate group appears [37,43,47]. In agreement, it was reported [48,49] that some chromates may give rise to dichromate-like IR spectra if they were bound to cations of a charge density as high as Cr, e.g. $Cr_2(CrO_4)_3$, $Tl_2(CrO_4)_3$, and $CdCrO_4$. Raising the calcination temperature up to 600°C, where the $Cr^{6+} \rightarrow Cr^{3+}$ reduction is affected either thermally (Eq. (9)) or chemically (Eq. (4)), one can observe an emergence of a very sharp two absorptions at 618 and 502 cm^{-1} which are assigned to the lattice vibration of chromite group [10,44]. Meanwhile, a weak absorption due to chromate ion is still evident. The picture is the same for the samples calcined at

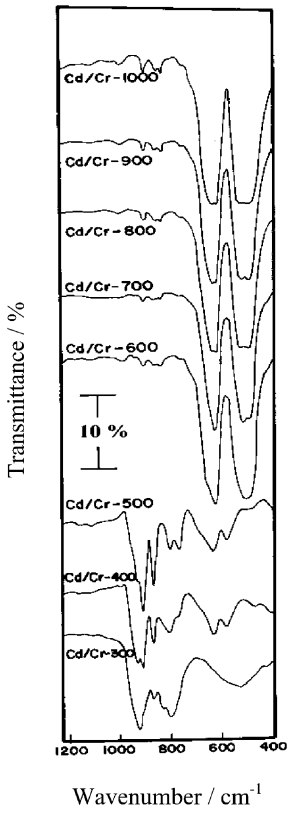

Fig. 5. FTIR spectra exhibited by the calcination products of the parent cadmium/chromia mixture in the temperature range 300–1000°C.

Table 3
Texture data of the calcination products of chromia gel as well as cadmium/chromia mixture

Calcination temperature (°C)	Cd/Cr-parent			Chromia gel		
	S_{BET} ($m^2\,g^{-1}$)	S_t ($m^2\,g^{-1}$)	Cr^{6+} ($mol\,m^{-2}$)	S_{BET} ($m^2\,g^{-1}$)	S_t ($m^2\,g^{-1}$)	Cr^{6+} ($mol\,m^{-2}$)
300	18.49	20.11	1.75E−4	153.91	142.32	2.27E−6
400	5.77	3.87	21.95E−4	30.77	30.94	4.71E−6
500	6.1	3.32	24.24E−4	25.29	25.14	4.31E−6
600	4.49	2.43	0.15E−4	21.7	20.79	4.01E−6
700	4.27	2.9	0.16E−4	10.41	10.31	3.84E−6
800	4.54	2.66	0.13E−4	10.93	10.38	2.29E−6
900	4.03	2.76	0.14E−4	5.26	5.16	2.09E−6
1000	2.79	2.32	0.11E−4	4.62	4.64	1.52E−6

700–1000°C temperature range. The only difference is that the band at 502 cm^{-1} suffers from a splitting into two bands located at 513 and 489 cm^{-1}. These spectra support the existence of cadmium chromite as a major phase in the 600–1000°C temperature range.

3.4. Determination of water extractable surface Cr^{6+} concentration

The results of colorimetric estimation of surface extractable Cr^{6+} ions for the calcination products of chromia gel as well as cadmium/chromia mixture are summarized in Table 3. In addition, the variation of Cr^{6+} concentration with the calcination temperature of both series is given in Figs. 6 and 7, respectively. Many authors [39,40,50–53] observed the phenomenon of oxidation of chromic oxide gel on heating in air. Deren et al. [50] assumed, therefore, that chromic oxide gel oxidized on heating to $Cr_2O_3{\cdot}3CrO_3$. Others [40,51] suggested the formation of chromium chromate. On the other hand, for the M–Cr–O systems (M = Ag^+, Zn^{2+}, Mg^{2+}, and Ni^{2+}), the detection of hexavalent chromium ions was attributed to the formation of metal chromates [8–10,36]. Generally, and according to the results given here, one can state safely that Cd/Cr catalysts possess much higher Cr^{6+} concentration than the corresponding Cr-ones. A fact that may reflect the stabilization role of cadmium ions to the high oxidation state of chromium ions throughout the formation of chromate species (cf. Table 2).

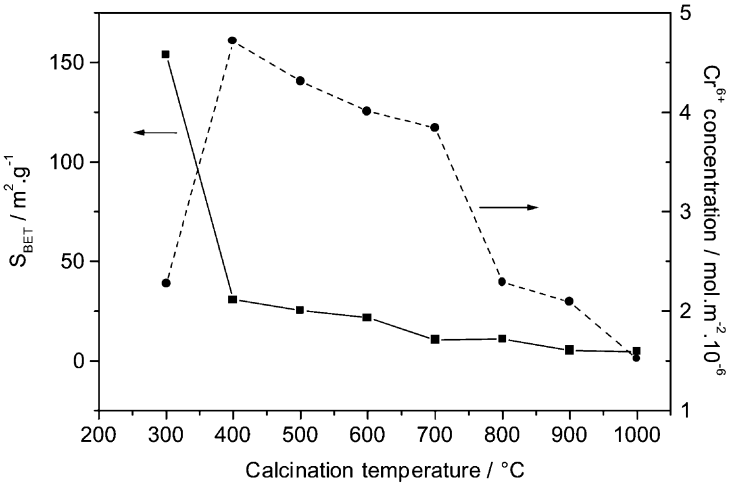

Fig. 6. Variation of the surface areas (S_{BET}) as well as the concentrations of surface Cr^{6+} of the Cr-*x* catalysts with the calcination temperature.

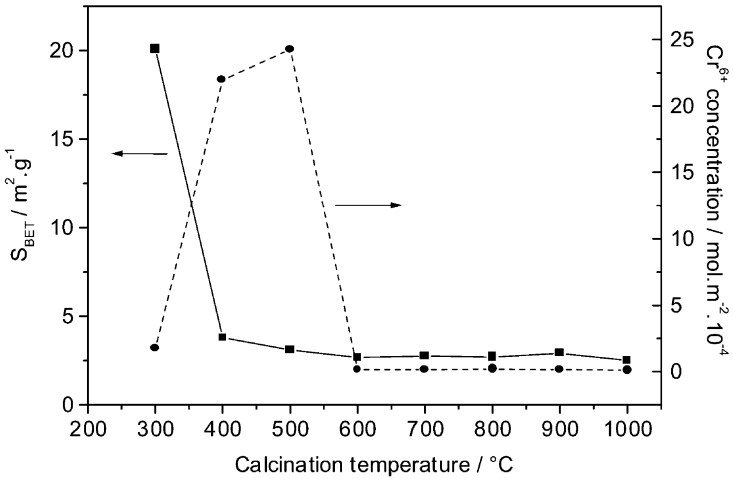

Fig. 7. Variation of the surface areas (S_{BET}) as well as the concentrations of surface Cr^{6+} of the Cd/Cr-*x* catalysts with the calcination temperature.

Upon heating the freshly-prepared chromia gel from 300 up to 1000°C, the water-leached Cr^{6+} ions increase firstly going from 300 to 400°C; showing a maximum value for Cr-400 sample; then decrease continuously till 1000°C. At 400°C we have two compensating processes: (i) decomposition of chromium oxide monohydrate (cf. XRD results), where the released water molecules leave back some chromium ions ready to coordinate with oxygen to the extent of Cr^{6+} formation; and (ii) crystallization of chromia into α-structure which is accompanied by a decrease in surface excess charge [52]. According to our results, we may suggest that the former effect predominates. Moreover, this mild increase in Cr^{6+} concentration may be correlated with the drastic drop in surface area values (vide infra), viz. 153.91 $m^2\,g^{-1}$ at 300°C and 30.77 $m^2\,g^{-1}$ at 400°C. Within this context, the continuous decrease in the Cr^{6+} values for the other chromium catalysts is a direct response to the α-Cr_2O_3 formation (which increases with increasing the calcination temperature) as well as the continuous decrease in the measured surface areas of these catalysts.

The detection of water extractable Cr^{6+} ions from the calcination products of cadmium/chromia parent mixture indicates that raising the calcination temperature from 300 up to 500°C is accompanied by a continuous increase in its concentration. Passing Cd/Cr-500 to Cd/Cr-600 catalyst resulting in a drastic drop of Cr^{6+} concentration. No marked change in Cr^{6+} concentration was observed as a result of raising the calcination temperature from 600 till 1000°C. These findings respond positively to the inference drawn from the XRD results, they confirm that the highest Cr^{6+} concentrations are observed in the temperature range where cadmium chromate represents the major phase, i.e. at 300–500°C.

3.5. Surface area measurements and grain morphology

Adsorption–desorption isotherms of nitrogen were measured on the calcination products of chromia gel as well as cadmium/chromia mixture. The sorption isotherms (not shown) were found to be of type II of Brunauer's classification [54]. The surface areas, calculated by applying the BET equation, are cited in Table 3. Moreover, the S_t values were also obtained using the V_a–*t* plots of de Boer and coworkers [24]. Figs. 6 and 7 report the surface area change as a function of the calcination temperature for chromia gel and cadmium/chromia mixture, respectively. Following up the variation of S_{BET} values of both series with calcination temperature two points can be raised: (i) the chromia-catalysts exhibited higher areas than the corresponding cadmium/chromium ones; and (ii) for both series, raising the calcination temperature from

300 up to 400°C is accompanied by a drastic drop in the measured S_{BET} values, whereas further raise in the heating temperature up to 1000°C produces the expected continuous decrease in the surface areas. The high surface areas for Cr-300 and Cd/Cr-300 catalysts can be reasonably correlated with the weight change of the starting parents as illustrated by TGA analysis. The evolved gases (H_2O from Cr-parent and H_2O, O_2, and NO_x from Cd/Cr-one) are responsible for the creation of new pore system having high surface areas. The drop in the surface areas of both series, as observed upon raising the calcination temperature from 300 up to 400°C, can be understood taking into account two factors: (i) sintering effect which increases with the temperature; and (ii) the presence of high concentration of Cr^{6+} ions at 400°C calcination products of both series. In this respect, it was reported, for chromium oxide [38] and for $ZnO:Cr_2O_3$ system [10], that the presence of such ions produce pore narrowing even to the extent of blocking and hence decreasing the surface area. Finally, the continuous decrease in the S_{BET} values, for both series, with the calcination temperature can be related to the process of densification, which is going parallel with the sintering process.

With the aid of electron microscopic investigations, it is possible to obtain further knowledge about the surface features of our catalysts. The microscopic investigations of chromia is given elsewhere [55]. Focusing our attention on Cd/Cr system, and with the aid of the previous analyses, selected three catalysts of this system were investigated, viz. Cd/Cr-500, Cd/Cr-600, and Cd/Cr-1000. The SEM micrograph of Cd/Cr-500 catalyst (Fig. 8a) showed spherical crystallites with size varying in the range 0.27–0.67 μm. Moreover, irregular holes distributed among the particles is evident. Raising the calcination temperature to 600°C, where $CdCr_2O_4$ formation starts, one can observe that Cd/Cr-600 catalyst (Fig. 8b) possesses the same morphological features as that of Cd/Cr-500 one, but with smaller grain size (0.07–0.53 μm) as well as smaller irregular holes. Inspection of Cd/Cr-1000 sample (Fig. 8c) revealed that this catalyst consisted of highly crystalline material with large particles (0.27–4 μm in size) having a well-defined edges. In view of our results, we can conclude that the perfect structure of cadmium chromite can be obtained by calcining the parent mixture at high temperatures as such as 1000°C.

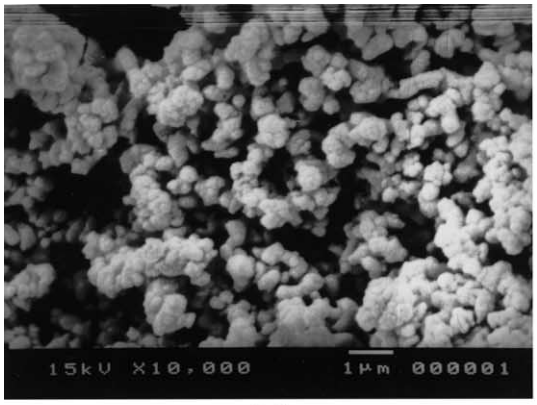

(a)

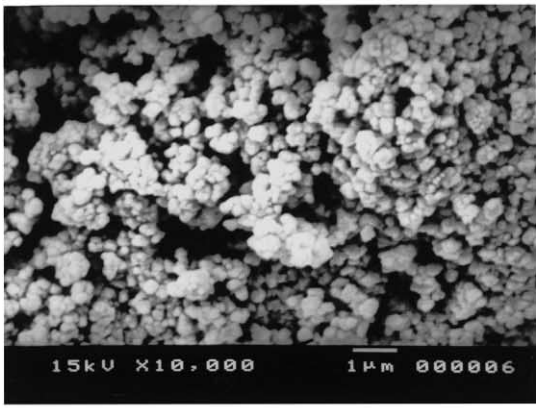

(b)

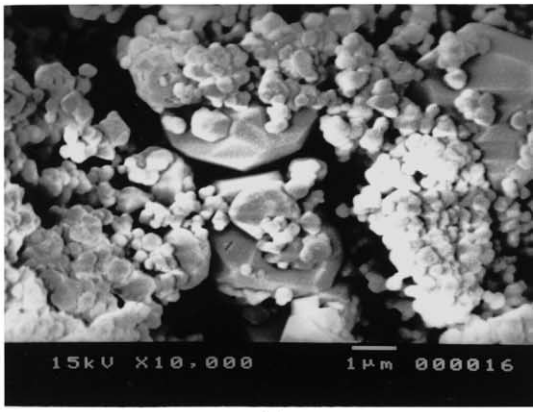

(c)

Fig. 8. SEM micrographs obtained for Cd/Cr-500 (a), Cd/Cr-600 (b), and Cd/Cr-1000 (c) catalysts.

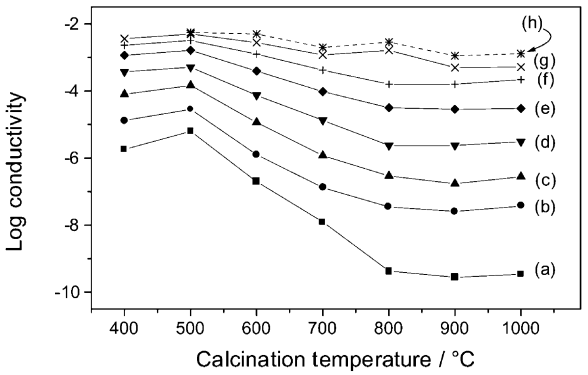

Fig. 9. Variation of $\log\sigma$ of the Cd/Cd-*x* catalysts with the calcination temperature, where the measurements were carried out at 100 (a), 150 (b), 200 (c), 250 (d), 300 (e), 350 (f), 400 (g), and 450°C (h).

3.6. Electrical conductivity measurements

Fig. 9 shows the variation of conductivity values, as obtained in air atmosphere at the 100–450°C temperature range, with the calcination temperature of the cadmium/chromia parent mixture. Considering the conductivity values at 100°C, it appears that the calcination products at 400°C are characterized by a higher specific conductivity value ($1.8\text{E}{-6}\,\Omega^{-1}\,\text{cm}^{-1}$), this value slightly increases upon raising the calcination temperature up to 500°C. Then, a continuous lowering of conductivity can be observed upon further increase of the calcination temperature up to 800°C which displays a specific conductivity of $4.35\text{E}{-10}\,\Omega^{-1}\,\text{cm}^{-1}$. At more elevated calcination temperatures, i.e. at 900 and 1000°C, almost the same conductivity values as for 800°C-products were also obtained. A combination between the above findings together with the results of TGA and XRD analyses allows us to consider the variation of conductivity values to reflect the accompanied structural changes of the parent mixture upon raising the heating temperature from 400 to 1000°C. Consequently, the higher conductivity values of Cd/Cr-400 and Cd/Cr-500 catalysts are mainly referred to the formation of α-Cr_2O_3 and α-$CdCrO_4$, and α-Cr_2O_3 and β-$CdCrO_4$ mixtures, respectively, whereas the subsequent formation of $CdCr_2O_4$ at temperatures higher than 500°C is accompanied by a noticeable lowering of conductivity. Such a lowering becomes greater with increasing the order of crystallinity of $CdCr_2O_4$ spinel which reaches almost a complete ordered form at 800°C. Then, heating the parent mixture at more elevated temperatures, i.e. at 900 and 1000°C, has no marked influence on the measured values. A situation that can be evidenced from the constancy of the conductivity values for the 800–1000°C calcination products.

A comparison between the mode of conductivity variations of the various samples with the estimated Cr^{6+} ions (Table 3) clearly indicates a parallel relationship between the conductivity increase and the Cr^{6+} content. Thus, the higher conductivity values characterizing Cd/Cr-400 and -500 catalysts can be ascribed to the co-existence of a large amount of Cr^{3+} – Cr^{6+} pairs forming a stable surface mobile-electron Zener phase [9]. The presence of such redox couple of chromium ions on the surface creates an ideal environment for maximization of the conductivity [10]. In a similar manner, the conductivity lowering observed for the calcination products of the parent Cd/Cr mixture at more elevated temperatures, i.e. above 500°C, can be related to the solid-state reaction given by Eq. (4) which acts to diminish the number of Cr^{3+}– Cr^{6+} pairs and, consequently, leads to such a conductivity lowering [56]. However, the above concept could explain the conduction behavior depending on the existence of pairs of chromium ions in two different oxidation states, the possibility of other participants to be exist and to have influence on the electrical behavior cannot be ignored. In this respect, it was stated [57], for chromia-containing catalysts, that there are sites having an excess positive charge (low anion charge) which seek to be neutralized by electron movement either from a negatively-bound entity or by electron movement from the bulk of the solid. Such electron movement will tend eventually to an increase of conductivity. It is to be noticed that one of the two constituents forming the parent Cd/Cr mixture is cadmium nitrate salt, which decomposes to cadmium oxide with the excess of cadmium in the bulk and the surface layers [58,59]. This excess cadmium is produced by the removal of the lattice oxygen [60] either from the bulk or from the surface and can be again ionized thermally, giving interstitial cadmium (II) cations and free electrons. Thus, an additional source of charge carriers will be created causing the observed higher conductivity values of Cd/Cr calcination products. The above explanation finds support when the

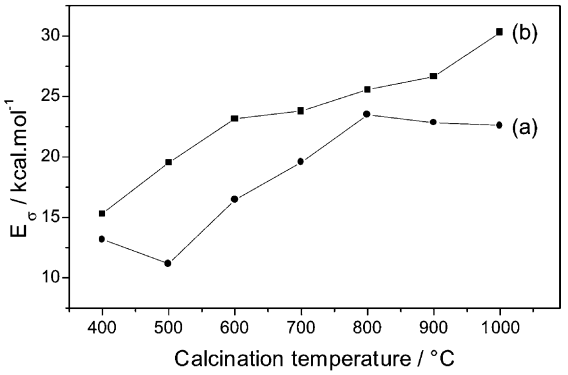

Fig. 10. Variation of the activation energy of conductance with the calcination temperature of Cd/Cr-*x* (a) and Cr-*x* (b) catalysts.

activation energies of conductance (E_σ), characterizing the calcination products of the parent chromia as well as Cd/Cr mixture, were calculated. Results are represented in Fig. 10 as a relationship between the E_σ values and the calcination temperature of the various samples. One can easily distinguish a remarkable lowering of E_σ values for Cd/Cr calcination products (curve a) compared to the corresponding cadmium-free samples (curve b). A situation confirms the suggested role of cadmium oxide in enhancing the conduction process of Cd/Cr system. In addition, it appears that the conductivity behavior of Cd/Cr system is divided to three regions depending on the calcination temperature, viz. 400–500, 500–800, and 800–1000°C regions. The calcination products in these temperature regions possess different activation energy values which arranged in the order $R_1 < R_2 < R_3$ (where R = region). It is evident from the XRD analysis that chromate–chromium oxide, disordered chromite–chromium oxide, and ordered chromite spinel are the phases formed in the above three regions, respectively. Thus, one can conclude that raising the calcination temperature of the parent Cd/Cr system is accompanied by an increase in the activation energy of conductance values and, consequently, a less charge carriers mobility.

4. Conclusions

1. The results of this study demonstrate the importance of understanding interactions between cadmium and chromium ions in the development of cadmium/chromia catalyst. In addition, catalyst preparation environment, e.g. air, nitrogen, and hydrogen, can have profound effects on the catalyst structure.
2. As it was shown for several transition metal chromates, e.g. copper chromate [33], zinc chromate [10], and silver chromate [36], the thermal stability of cadmium chromate, in air atmosphere, is limited to 500°C. At more elevated temperatures, cadmium chromite spinel forms.
3. The step formation of the intermediate chromate is hindered in hydrogen atmosphere, while retarded when curing medium is nitrogen. This indicates that oxygen is necessary for this intermediate formation and hence for the spinel itself. In this regard, it is plausible to suggest that the limited supply of oxygen resulting from lateral hydroxyl groups condensation of chromia gel partner [38] taking place during heating up the starting mixture contributes to oxidation and, hence, cadmium chromate formation.
4. From the electrical conductivity measurements, it is evident that the charge carrier movements become easier for the 400–500°C calcination products of cadmium/chromia catalysts. Such property will have a marked influence on the catalytic behavior of these catalysts, as it will be discussed in the next paper.

References

[1] B. Grzybowska, J. Słoczyński, R. Grabowski, K. Wciło, A. Kozłowska, J. Stoch, J. Zieliński, J. Catal. 178 (1998) 687.
[2] D.W. Flick, M.C. Huff, Appl. Catal. A 187 (1999) 13.
[3] J.H. Uhm, M.Y. Shin, J. Zhidong, J.S. Chung, Appl. Catal. B 22 (1999) 293.
[4] H.G. El-Shobaky, A.M. Ghozza, G.A. El-Shobaky, G.M. Mohamed, Colloids Surf. A 152 (1999) 315.
[5] B.M. Weckhuysen, R.A. Schoonheydt, Catal. Today 51 (1999) 215.
[6] N.E. Fouad, H. Knözinger, M.I. Zaki, S.A.A. Mansour, Z. Phys. Chem. 171 (1991) 75.
[7] G. Busca, J. Catal. 120 (1989) 303.
[8] R.B. Fahim, M.I. Zaki, A.M. El-Roudi, A.M.A. Hassaan, J. Res. Inst. Catal., Hokaido Univ. 29 (1981) 25.
[9] R.M. Gabr, M.M. Girgis, A.M. El-Awad, Mater. Chem. Phys. 30 (1992) 169.
[10] R.M. Gabr, M.M. Girgis, A.M. El-Awad, B.M. Abou-Zeid, Mater. Chem. Phys. 39 (1994) 53.

[11] B.M. Abu-Zied, M.Sc. Thesis, Assiut University, Assiut, 1994.
[12] B.A. Marinkovic, Z.V. Zakula, T. Sreckovic, M. Tomasevic, M.M. Ristic, Cryst. Res. Technol. 34 (1999) 881.
[13] M. Catti, F.F. Fava, C. Zicovich, R. Dovesi, Phys. Chem. Miner. 26 (1999) 389.
[14] L. Forni, J. Catal. 111 (1988) 199.
[15] S.R. Naidu, A.K. Banerjee, N.O. Ganguli, S.P. Sen, J. Res. Inst. Catal., Hokkaido Univ. 21 (1973) 172.
[16] M. Bertoldi, B. Fubini, E. Giamello, G. Busca, F. Trifiro, A. Vaccari, J. Chem. Soc., Faraday Trans. 1 84 (1988) 1405.
[17] E. Giamello, B. Fubini, M. Bertoldi, G. Busca, A. Vaccari, J. Chem. Soc., Faraday Trans. 1 85 (1989) 237.
[18] G.B. Hoflund, W.S. Epling, D.M. Minahan, Catal. Lett. 62 (1999) 169.
[19] J.M. Arandes, J. Erena, A.G. Gayubo, J. Bilbao, H.I. De Lasa, Chem. Eng. Commun. 174 (1999) 1.
[20] B.M. Reddy, I. Ganesh, J. Mol. Catal. A 151 (2000) 289.
[21] L. Lietti, E. Tronconi, P. Forzatti, J. Catal. 135 (1992) 400.
[22] N.N. Greenwood, A. Earnshaw, Chemistry of the Elements, Pergamon Press, New York, 1984, p. 1400.
[23] D.N. Trifonov, V.D. Trifonov, Chemical Elemennts: How They Were Discovered, Mir Publishers, Mosco, 1985, p. 101.
[24] B.C. Lippens, B.G. Linsen, J.H. de Boer, J. Catal. 3 (1964) 32.
[25] M.M. Girgis, J. Mater. Sci. 28 (1993) 4925.
[26] P.R. Chapman, R.H. Griffith, J.D.F. Marsh, Proc. R. Soc. (London) 224 (1954) 419.
[27] F.S. Baker, J.D. Carruthers, R.E. Day, K.S.W. Sing, L.J. Stryker, Diss. Faraday Soc. 52 (1971) 173.
[28] D.L. Mayers, J.H. Lunsford, J. Catal. 92 (1985) 620.
[29] W.F. McClune (Ed.), Powder Diffraction File (Inorganic Compounds), Joint Committee on Powder Diffraction Standards, Swarthmore, PA, 1983.
[30] F.A. Cotton, G. Wilkinson, Advanced Inorganic Chemistry, Wiley, New York, 1980, p. 589.
[31] M.A.A. Beg, M.A. Qaiser, Thermochim. Acta 173 (1990) 281.
[32] A.M.M. Gadalla, Thermochim. Acta 74 (1984) 255.
[33] F. Hanic, I. Horvath, G. Plesch, J. Gàlikovà, J. Solid State Chem. 59 (1985) 190.
[34] Z. Tianshu, P. Hing, Z. Jiancheng, K. Lingbing, J. Mater. Chem. Phys. 61 (1999) 192.
[35] C. Cantalini, M. Faccio, G. Ferri, M. Pelino, Sens. Actuators B 15/16 (1993) 193.
[36] B.M. Abu-Zied, Appl. Catal. A 198 (2000) 139.
[37] M.I. Zaki, R.B. Fahim, J. Thermal Anal. 31 (1986) 825.
[38] R.B. Fahim, R.M. Gabr, M.I. Zaki, S.A.A. Mansour, J. Colloid Inter. Sci. 81 (1981) 468.
[39] R.B. Fahim, M.I. Zaki, N.H. Yacoub, J. Colloid Inter. Sci. 88 (1982) 502.
[40] R.Sh. Mikhail, S.A. Selim, J. Appl. Chem. Biotechnol. 24 (1974) 557.
[41] I.P. Saraswat, A.G. Vajpei, J. Mater. Sci. Lett. 3 (1984) 515.
[42] D.A. Brown, D. Cunningham, W.K. Glass, Spectrochim. Acta 24A (1968) 965.
[43] F.A. Miller, C.H. Wilkins, Anal. Chem. 24 (1952) 1253.
[44] R.A. Nyquist, R.O. Kagel, Infrared Spectra of Inorganic Compounds, Academic Press, London, 1971, pp. 13–16.
[45] P.J. Miller, G.L. Cessac, R.K. Khanna, Spectrochim. Acta 27A (1971) 2091.
[46] O. Muller, W.B. White, R. Roy, Spectrochim. Acta 25A (1969) 1491.
[47] H. Stammreich, D. Bassi, O. Sala, N. Siebert, Spectrochim. Acta 13 (1958) 192.
[48] M.I. Zaki, N.E. Fouad, J. Leyer, H. Knözinger, Appl. Catal. 21 (1986) 359.
[49] J.A. Campell, Spectrochim. Acta 21 (1965) 1333.
[50] J. Deren, J. Haber, A. Podgorecka, J. Burzyk, J. Catal. 2 (1963) 161.
[51] J.D. Curruthers, K.S.W. Sing, J. Fenerly, Nature 213 (1976) 135.
[52] R.B. Fahim, R.M. Gabr, M.I. Zaki, Colloids Surf. 6 (1983) 135.
[53] R.B. Fahim, K.M. Abd-El-Salaam, M.E. Ahmed, Bull. Fac. Sci., Assiut Univ. 6 (1977) 159.
[54] P.A. Webb, C. Orr, Analytical Methods in Fine Particles Technology, Micromeritics Instrument Corp., Norcross, 1997, p. 55.
[55] N.E. Cross, F.H. Leach, J. Catal. 21 (1971) 239.
[56] M.M. Girgis, A.M. El-Awad, J. Mater. Chem. Phys. 36 (1993) 48.
[57] J.C. Vickerman, J. Catal. 44 (1976) 404.
[58] R.B. Fahim, K.M. Abd-El-Salaam, Z. Phys. Chem. 85 (1973) 287.
[59] R.B. Fahim, K.M. Abd-El-Salaam, Z. Phys. Chem. 91 (1974) 263.
[60] E.F. Lamp, F.C. Tompkins, Trans. Faraday Soc. 58 (1962) 1424.